Supplementary Data

LAP-TLR2 Axis Drives Inflammatory Pathology during *Listeria monocytogenes* Gastroenteritis

Dongqi Liu et al.

Corresponding Author: Arun Bhunia (bhunia@purdue.edu)

Supplementary Tables

Supplementary Table 1. Gastroenteritis outbreak-causing *Listeria monocytogenes* strains used in this study.

Strain	Year	Outbreak Associated	Location	Serotype	CC*	Source	Assembly
G4599	1993	Yes	Italy	1/2b	CC59	Human	JPTX00000000
G4600	1993	Yes	Italy	1/2b	CC59	NA	PDT000158612.2
G6006	1994	Yes	USA	1/2b	CC3	Food (chocolate milk)	ASM2131255v1
G6054	1994	Yes	USA	1/2b	CC3	Human (stool)	ASM341783v1
H7013	1997	Yes	Italy	4b	CC2	Food (cold salad of corn & tuna)	PDT000158606.2
H7014	1997	Yes	Italy	4b	CC2	Human (stool & blood)	PDT000158626.2
F4244	1991	Yes	USA	4b	CC6	Human (CSF)	ASM274091v1

*Clonal Complex (CC) number is determined by Pasteur MLST ST. BIGSdb-Lm platform (http://bigsdb.pasteur.fr/listeria/)

Supplementary Table 2. *Listeria* genotypes and their growth conditions

Listeria monocytogenes	**Genotype**	**Antibiotics used**	**Growth temperature**
F4244	WT	-	37°C
	lap^{-}	Em5	42°C
	lap^{-} *lap*$^{+}$	Em5, Cm5	42°C
	Δ*inlA*	-	37°C
	mInlA (murine InlA)	-	37°C
	mInlA lap^{-}	Em5	42°C
10403S	Δ*hly*	-	37°C
H7014	WT	-	37°C
	lap^{-}	Em5	42°C
	lap^{-} *lap*$^{+}$	Em5, Cm5	42°C
G4600	WT	-	37°C
G6006	WT	-	37°C
G6054	WT	-	37°C
H7013	WT	-	37°C

*Em5, 5 µg/mL of erythromycin; Cm5, 5 µg/mL of chloramphenicol.

Supplementary Table 3. Bacterial mutant strains, antibodies, cell lines, primers and reagents

REAGENT or RESOURCE	SOURCE	IDENTIFIER
Bacterial Strains		
L. monocytogenes F4244 serovar 4b (WT), CC6	Our collection [1]	N/A
L. monocytogenes F4244 *lap*$^{-}$ (isogenic *lap* insertion mutant)	Kim et al., 2006 [2]	N/A
L. monocytogenes F4244 *lap*$^{-}$ *lap*$^{+}$ (*lap* complemented)	Kim et al., 2006 [2]	N/A
L. monocytogenes F4244 Δ*inlA* (in-frame deletion)	Burkholder and Bhunia, 2010 [3]	N/A
L. monocytogenes F4244 *mInlA* (murinized InlA strain)	Bai et al. 2021 [4]	N/A
L. monocytogenes F4244 *mInlA lap*$^{-}$ (isogenic *lap* insertion mutant in murinized InlA background)	Drolia et al. 2024 [5]	N/A
Listeria monocytogenes 10403S Δ*hly* (in-frame deletion)	Glomski et al. 2003 [6]	DP-L2161
L. monocytogenes H7014 serovar 4b (WT), CC2, Italy, 1997	CDC	N/A
L. monocytogenes H7014 *lap*$^{-}$ (isogenic *lap* insertion mutant)	This study	N/A
L. monocytogenes H7014 *lap*$^{-}$ *lap*$^{+}$ (*lap* complemented)	This study	N/A
L. monocytogenes H7013 serovar 4b, Italy, 1997	CDC	N/A
L. monocytogenes G4600 serovar 1/2b, Italy, 1993	CDC	N/A
L. monocytogenes G6006 serovar 1/2b, USA, 1994	CDC	N/A
L. monocytogenes G6054 serovar 1/2b, USA, 1994	CDC	N/A
E. coli DH5α pMSG101-LAP	[7]	N/A
E. coli DH5α pAUL-AAD	[7]	N/A
Mammalian Cell Lines		
Caco-2	ATCC	Cat# HTB37
HEK-Blue-Lucia hTLR2 cell	Invivogen	hkd-htlr2ni
Antibodies		
Mouse monoclonal α-LAP (EM-H7)	Our Lab [8]	NA
Rabbit polyclonal α-InlA	Our Lab [3]	NA
Rabbit polyclonal α-InlB (Lm404)	Our Lab [9,10]	NA
Rabbit polyclonal α-LLO	This study	NA
Goat anti-rabbit HRP-conjugated IgG	Cell Signaling Technology	Cat # 7074, RRID: AB_2099233
Horse anti-mouse HRP-conjugated IgG	Cell Signaling Technology	Cat # 7076, RRID: AB_330924
α-CD90.2 (Thy1.2)-Pacific Blue	Biolegend	Cat#105323
α-CD45-BV711	Biolegend	Cat#103147
α-Ly6G-AlexaFluor488	Biolegend	Cat#127625
α-EpCAM (CD326)-PerCP Cyanine5.5	Biolegend	Cat#118219
α-B220 (CD45R)-PE	Biolegend	Cat#103207
α-CCR2-PE Cyanine 5	Biolegend	Cat#150637
α-Ly6C-PE Cyanine 7	Biolegend	Cat#128017
α-CD11c-APC	Biolegend	Cat#117309
eFluor 780 (Viability Dye)	eBioscience	Cat#65-0865-14

Commercial Reagents and Chemicals		
Pierce™ BCA Protein Assay Kit	Thermo Fisher	Cat# 23225
Halt™ Protease Inhibitor Cocktail (100X)	Thermo Fisher	Cat# 78429
PMSF Protease Inhibitor	Thermo Fisher	Cat# 36978
Halt™ Protease and Phosphatase Inhibitor Cocktail (100X)	Thermo Fisher	Cat# 78440
M-PER™ Mammalian Protein Extraction Reagent	Thermo Fisher	Cat# 78501
Phusion® High-Fidelity DNA Polymerase	NEB	Cat# M0530
Mouse Lipocalin-2/NGAL Duoset ELISA	R&D	Cat# DY1857
Fluorescent isothiocyanate-dextran 4 kDa	MillporeSigma	Cat# FD4
Fluorescent isothiocyanate-dextran 40 kDa	MillporeSigma	Cat# FD40
Fluorescent isothiocyanate-dextran 70 kDa	MillporeSigma	Cat# FD70
RNAlater	Thermo Fisher	Cat# AM7021
TL2-C29 (TLR2 Inhibitor)	Invivogen	Inh-c29
Modified Oxford agar Base	Neogen Corporation	Cat# 7428
Modified Oxford agar Base supplement	Neogen Corporation	Cat# 7991
Buffered Listeria enrichment broth	Neogen	Cat# 7675
Buffered Listeria enrichment broth supplement	Neogen	Cat# 7980
BD Microgard™ Gold	BD	Cat# 365967
Oligonucleotides		
LAP_NcoI_F CGCCCATGGCAATTAAAGAAAATGC	This study	N/A
LAP_XhoI_R CGCCTCGAGTTAAACACCTTTGTAAG	This study	N/A
mNHE2_F GGACACTGGGGTCACAACTT	This study	N/A
mNHE2_R GCGGTTTGAGCTGTTGTCTT	This study	N/A
mNHE3_F CCTTCATTCGCTCCCCAAGT	This study	N/A
mNHE3_R GTGTTAGCTCGTGCCGACTA	This study	N/A
mSGLT1_F TTCCAGACGTGCACCTGTAC	This study	N/A
mSGLT1_R GCACACTGGCTTCAAATGCA	This study	N/A
mDRA_F ACGAACATCGCAGACCTTGT	This study	N/A
mDRA_R TGTAGCGGCTGCAGAAGAAA	This study	N/A
mCLCA1_F GAATGAACCCACCACGTCCT	This study	N/A
mCLCA1_R TTGAGTCTTCGGGAATGGGC	This study	N/A
mCFTR_F AAAGTTGTCAAGCCGCGTTC	This study	N/A
mCFTR_R TATCTGTACGGCAGTGGGGA	This study	N/A
mNKCC1_F GGCTGCGTTGCTCACATATG	This study	N/A
mNKCC1_R GGCGGATAACCACAACTCCA	This study	N/A
mGAPDH_F TTCACCACCATGGAGAAGGC	This study	N/A
mGAPDH_R TGAAGTCGCAGGAGACAACC	This study	N/A
Analysis Software		
ImageJ	NIH	Ver 1.53k
GraphPad Prism	Graph Pad	Version 8.4.3
SnapGene	GSL Biotech	Version 6.0.2
Proksee	Genome Canada/Genome Alberta	NA

Supplementary Figures

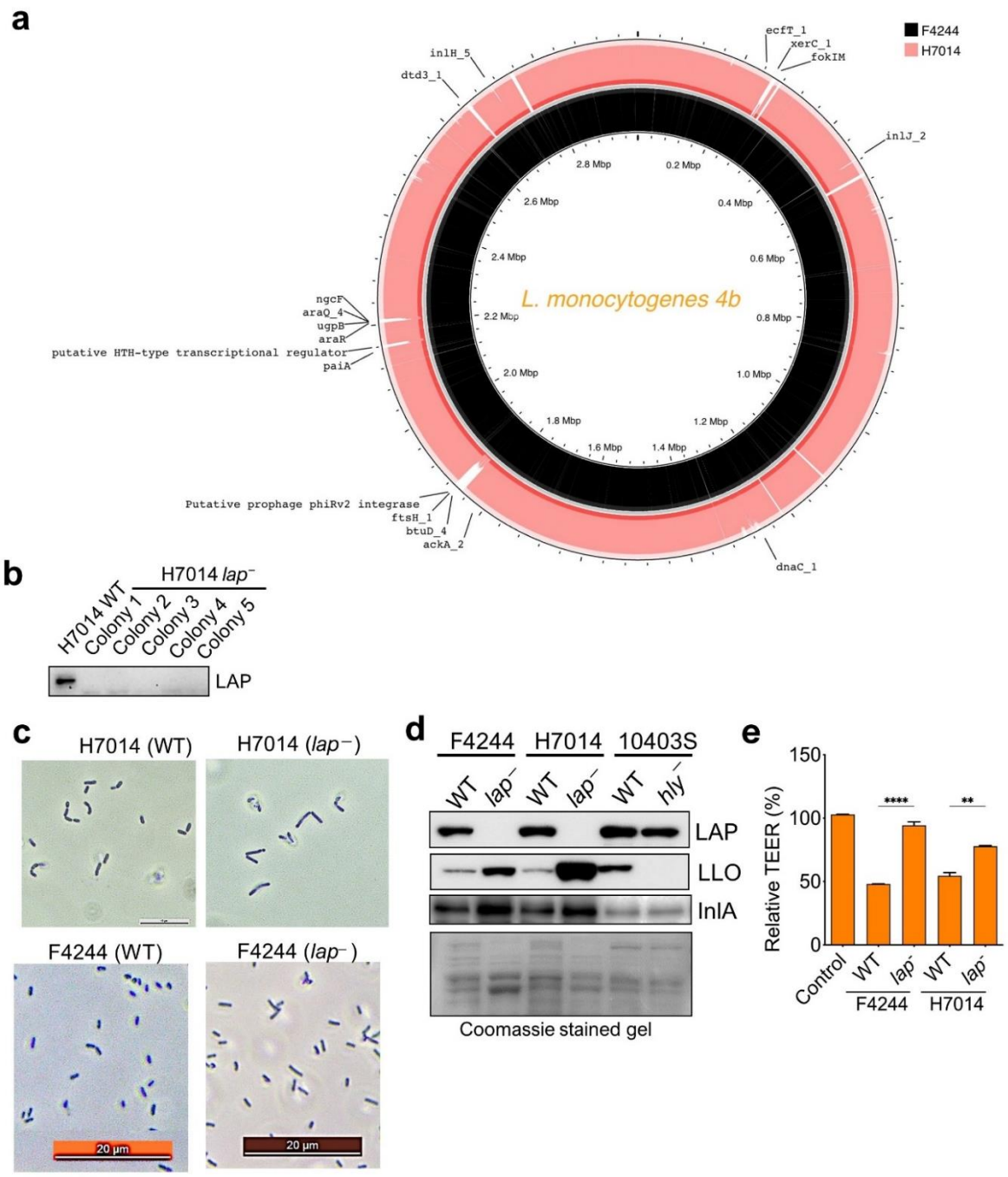

Supplementary Figure 1. LAP Mediates Epithelial Barrier Disruption and Lm Translocation by Expanding Paracellular Gap

a. Circular genomic alignment and comparative genomics between Lm F4244 (Black) and H7014 (Pink). **b,c.** Immunoblot (b) and microscopic morphology (c) characterization of the isogenic *lap*-deficient strain generated from the H7014 background. **d.** Immunoblots of LAP, InlA, and LLO levels in Lm WT, *lap*⁻ strains (F4244 and H7014 backgrounds). Lm 10403S WT and *hly*⁻ (hemolysin-deficient) strains serve as

positive and negative controls for LLO expression, respectively. Coomassie blue staining of total protein was used as a loading control. **e.** Relative TEER values after exposure to bacteria in a Transwell setup.

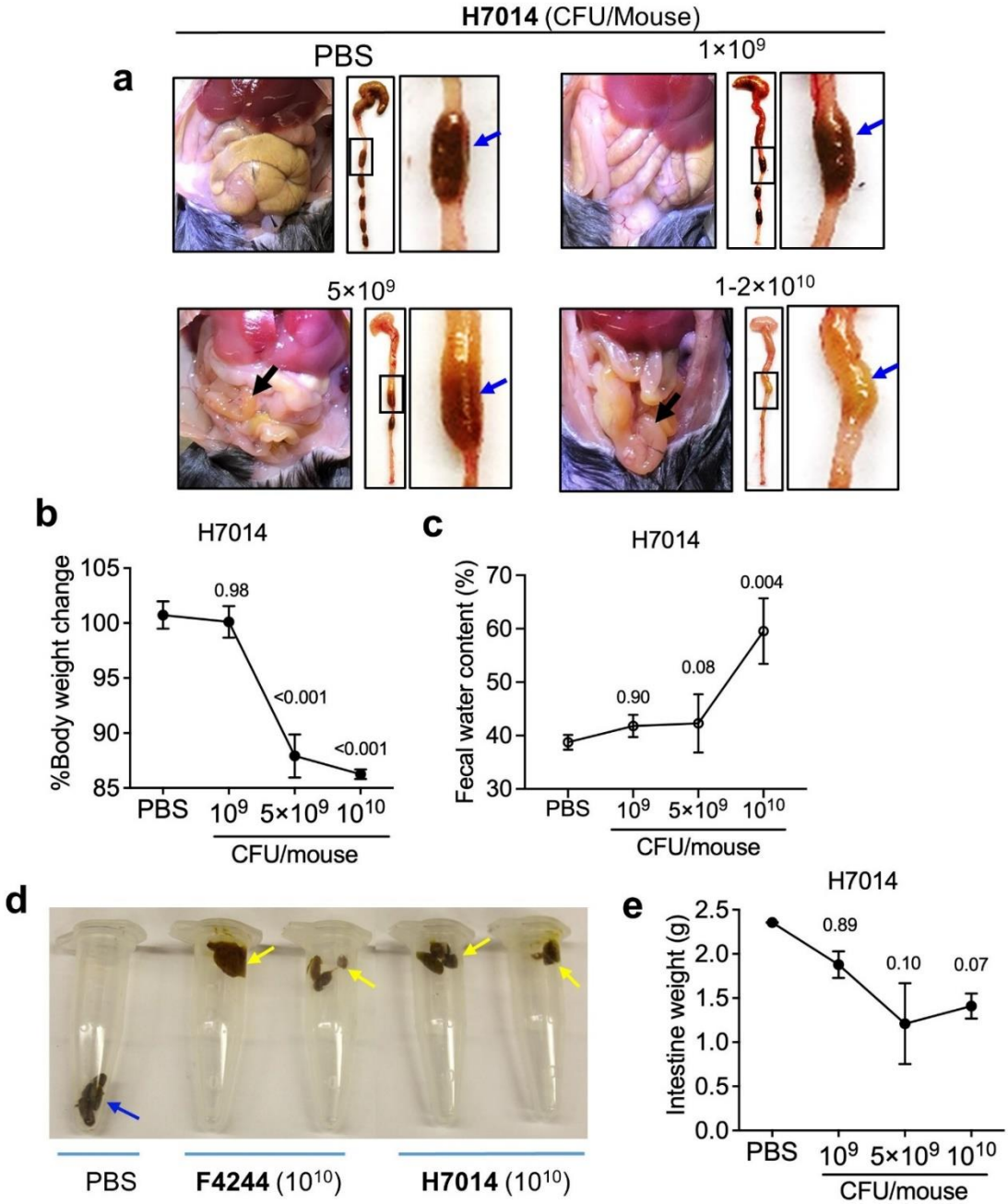

Supplementary Figure 2. Acute Gastroenteritis in mice gavaged with Lm.

a. Representative images of gross intestinal pathology of C57BL/6 WT mice that were intragastrically infected with 1 x 10^9, 5 x 10^9, 1-2 x 10^{10} CFU/mouse of Lm H7014, or PBS (Mock). **b.** Percentage change in total body weight. **c.** Analysis of fecal water content. PBS: n=6, Lm-infected mice: n=12-15

d. Fecal consistency (stickiness) after dosing with 1-2 x 10^{10} CFU/mouse of F4244 and H7014 after 48 hpi. **e.** Intestinal weight of mice infected with Lm H7014 after 48 h. n=5-6. All error bars represent SEM, marked with P values. All experiments were repeated at least three times unless otherwise noted.

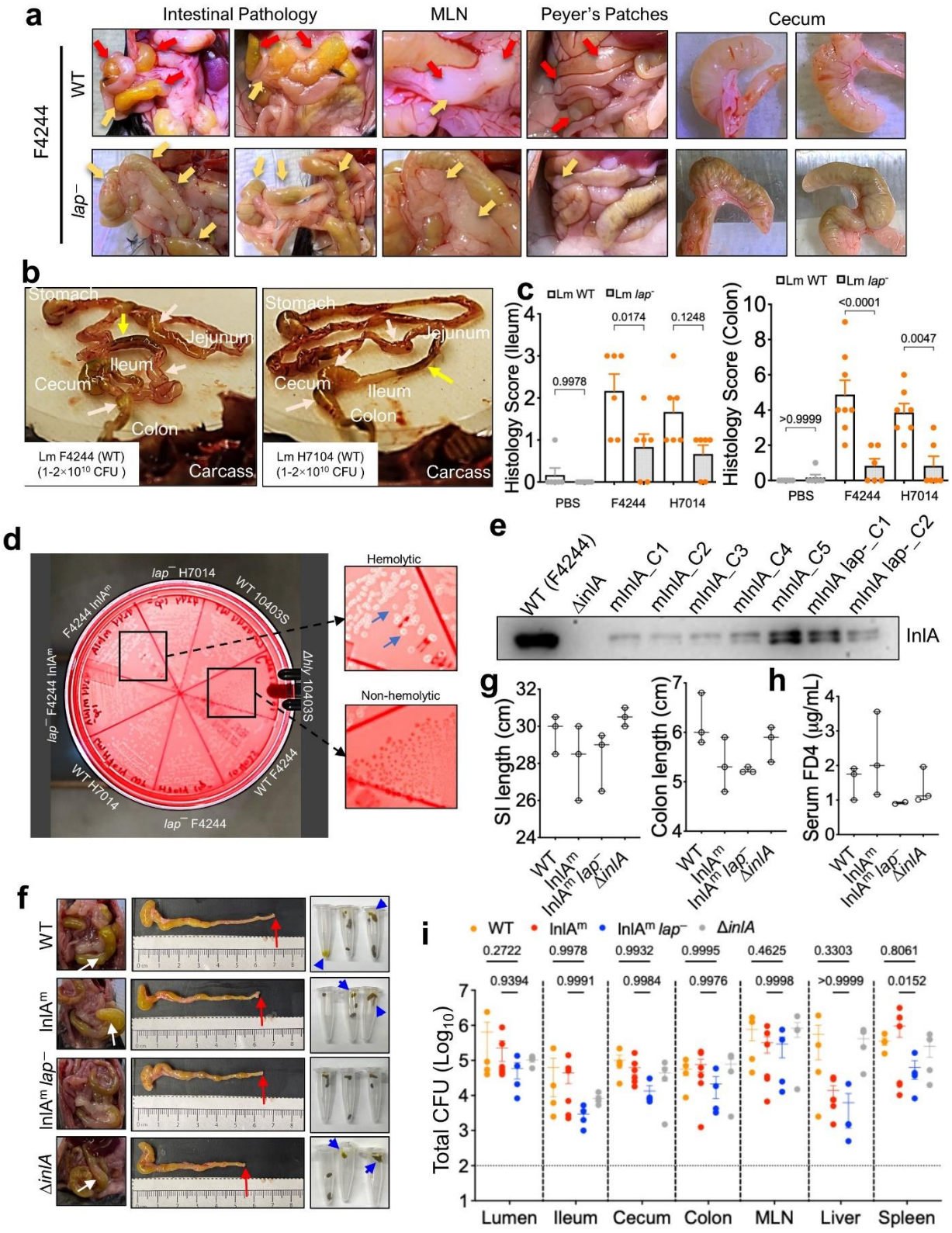

Supplementary Figure 3. LAP is the Main Driver of Gastroenteritis In Vivo.
a. Representative images of gross intestinal pathology and close-up images of mesenteric lymph nodes (MLN), Peyer's patches, and cecal contents from mice infected with Lm F4244 WT or *lap*$^{-}$.
b. Representative images of the whole intestine from stomach to colon infected with Lm F4244 WT or *lap*$^{-}$.
c. Intestinal histopathological scores of Lm WT or *lap*$^{-}$ in both F4244 and H7014 backgrounds.
d. Characterization of Lm isolates and variants on blood agar. All tested strains, with the exception of the10403S Δ*hly*, exhibited clear zones of β-hemolysis (blue arrows from zoom-in image).
e. Immunoblot confirming InlA expression in F4244 InlA^{m} and InlA^{m} *lap*$^{-}$ strains. F4244 WT and ΔinlA serve as positive and negative controls, respectively.
f-i. Assessment of gross intestinal pathology and fecal morphology (f), small and colon length of mice infected with Lm F4244 WT, InlA^{m}, InlA^{m} *lap*$^{-}$, ΔInlA (g), serum FD4 permeability (h), and tissue Lm burdens (i) in mice infected with Lm InlA variants. The symptoms of InlA^{m} *lap*$^{-}$ are less intense, characterized by visible pellet structure (chunks) rather than watery stool; reduced mucus residues on the pellets compared to WT and InlA^{m} (blue arrows). B6 mice were intragastrically gavaged with 1-2 x 10^{10} CFU/mice Lm F4244 WT, murinized InlA (InlA^{m}), InlA^{m} *lap*$^{-}$, and ΔInlA.

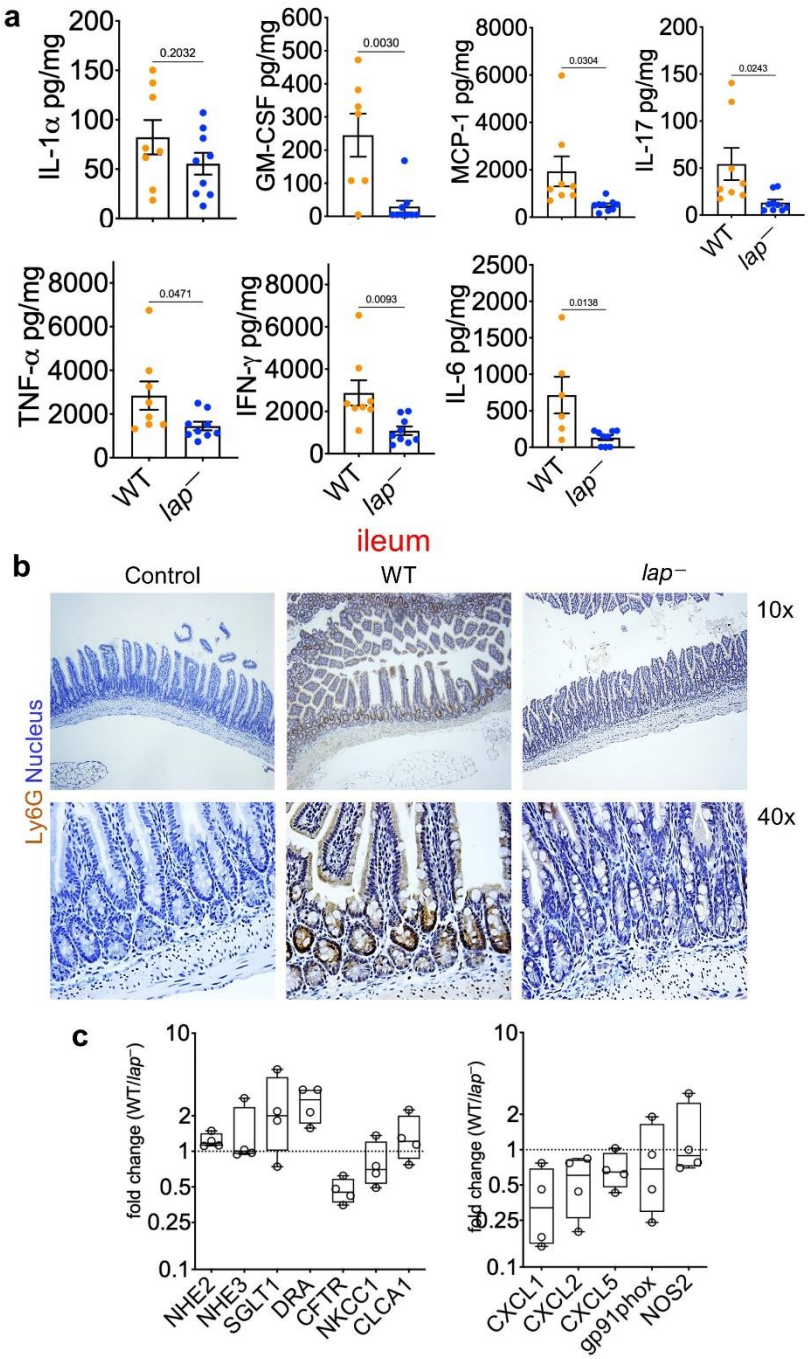

Supplementary Figure 4. LAP-induced leaky gut exacerbates gastroenteritis symptoms through increased epithelial cell death and immune cell infiltration

a. Colonic proinflammatory cytokine profiling of mice infected with Lm H7014 WT and Lm H7014 *lap*−. **b.** Representative IHC staining for Ly6G (brown) in the ileum. Lm background is F4244. **c**. Relative mRNA levels of ion absorptive/secretory ion channels for Lm WT/ *lap*−.

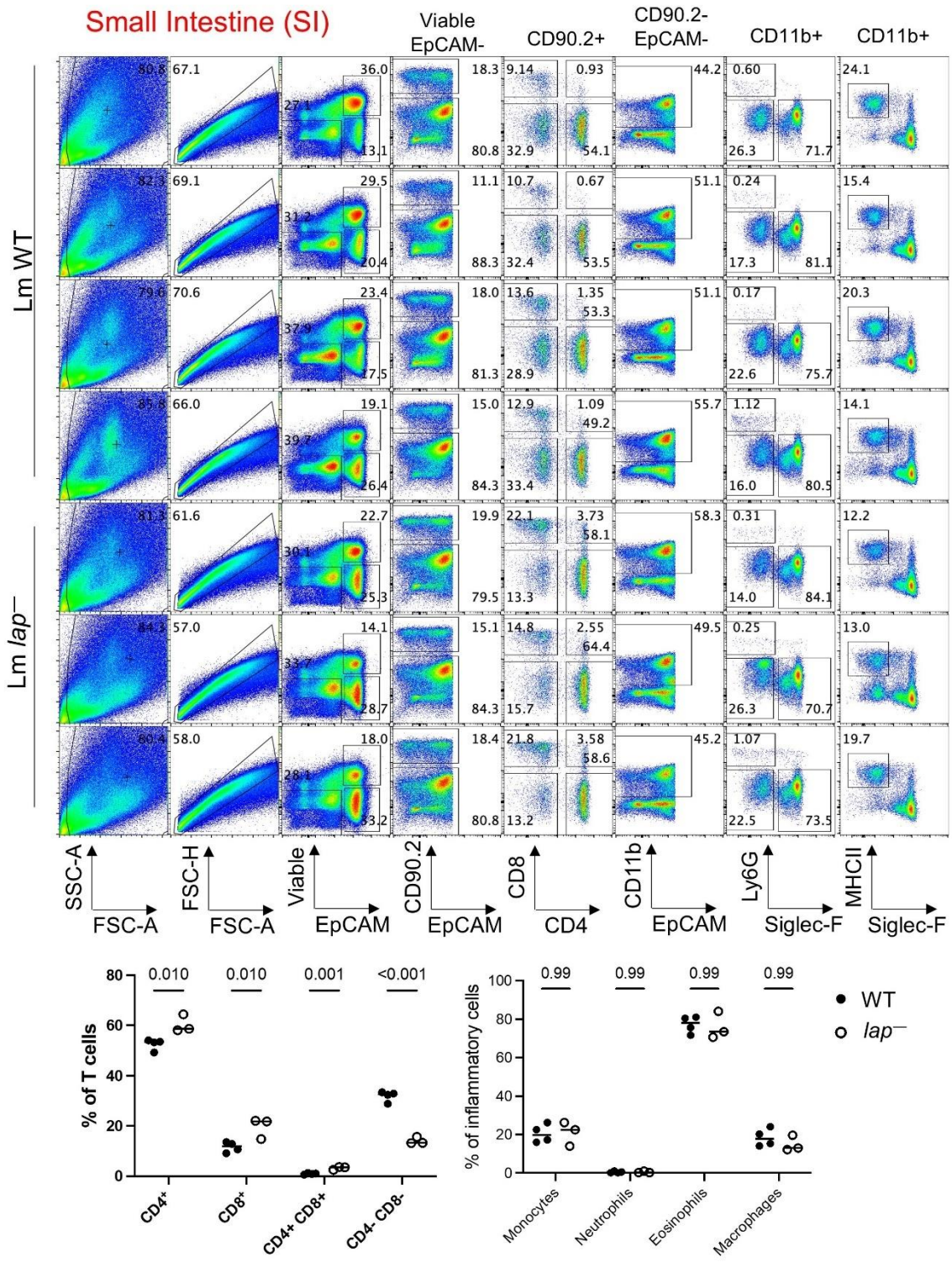

Supplementary Figure 5. LAP-induced leaky gut exacerbates gastroenteritis symptoms through increased epithelial cell death and immune cell infiltration. Flow cytometry gating strategy and immune cell subset frequencies in the small intestine. B6 mice were infected with Lm F4244 WT or Lm F4244 *lap*⁻ at 1-2 x10^{10} CFU/mouse.

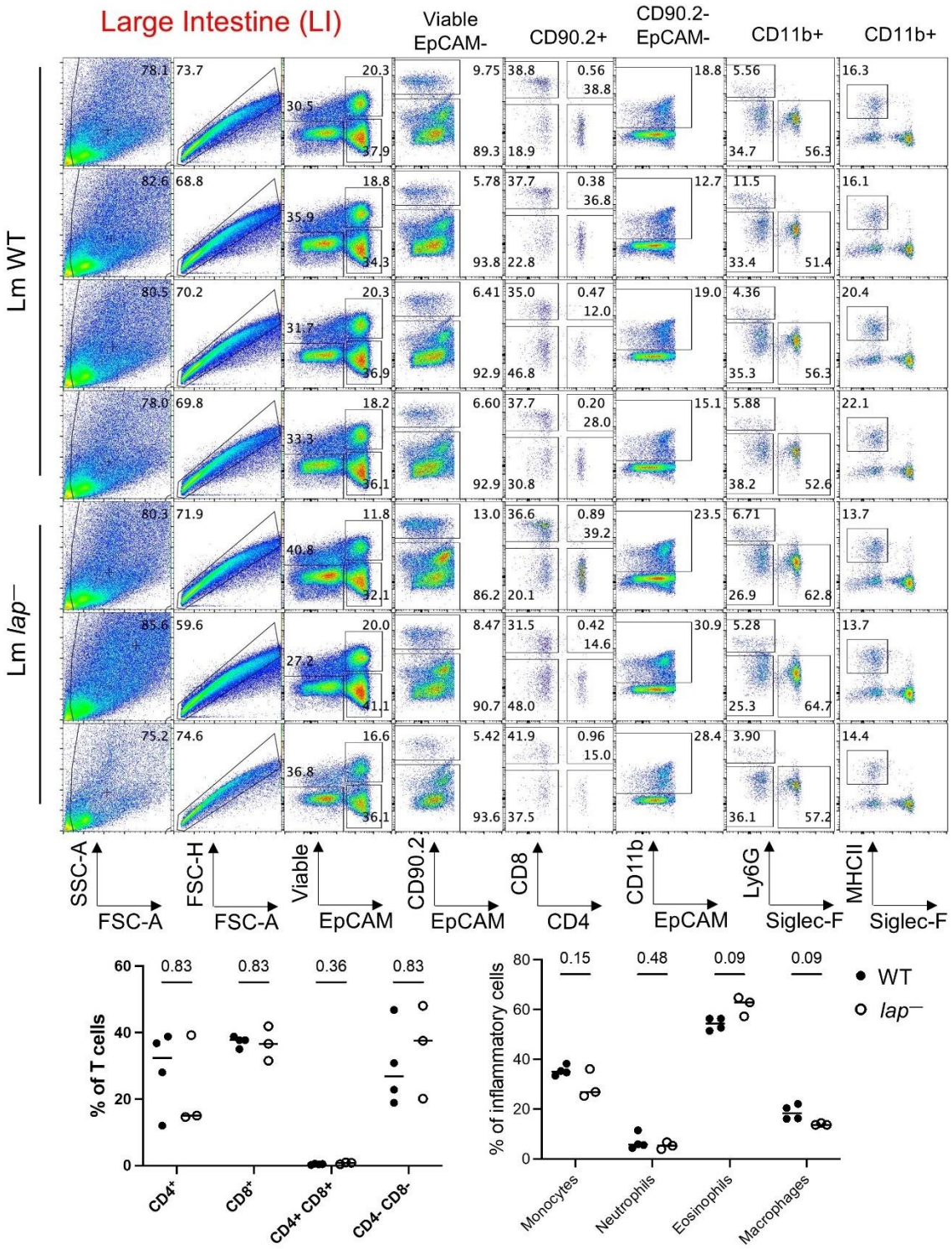

Supplementary Figure 6. LAP-induced leaky gut exacerbates gastroenteritis symptoms through increased epithelial cell death and immune cell infiltration. Flow cytometry gating strategy and immune cell subset frequencies in the large intestine. B6 mice were infected with Lm F4244 WT or Lm F4244 *lap*⁻ at 1-2 x10^{10} CFU/mouse.

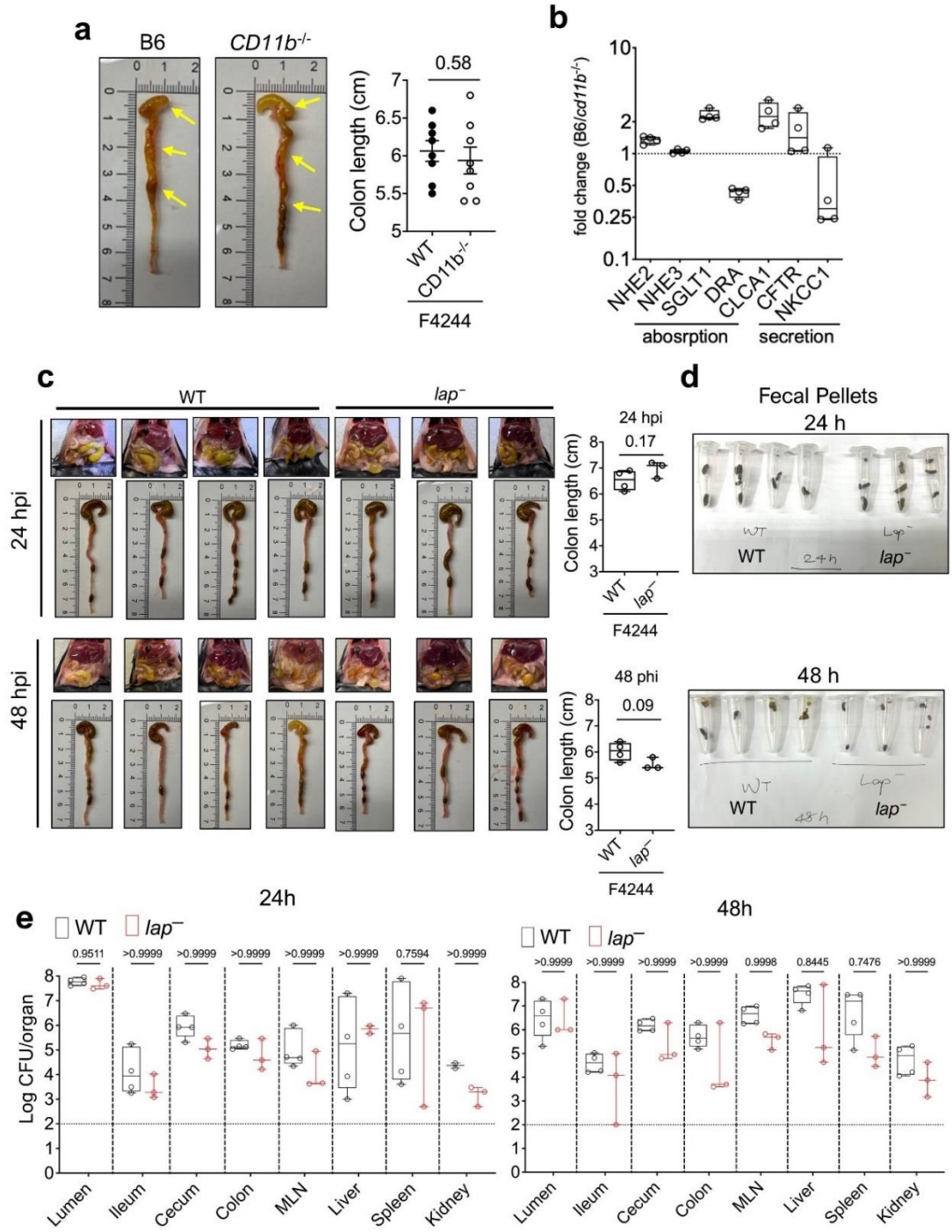

Supplementary Fig 7. CD11b^{+} Myeloid Cells Mediate Diarrheal Symptoms and Contain Lm Spread in the intestine.

a. Representative images and corresponding bar plots showing the length of the small (a)(stomach-ileum) and large intestine (b)(cecum-colon). Percentage of viable colonic IEC cells from Lm-infected B6 and Cd11b$^{-/-}$ mice. **b.** Relative mRNA level of ion absorptive/secretory ion channels and Ca^{2+} dependent ion channel regulator from the ileum. **c.** Gross intestinal pathology and cecum-colon length of *CD11b*$^{-/-}$mice infected with 1 x 10^{10} CFU/mouse F4244 Lm WT or *lap*$^{-}$at 24 and 48 hpi. Colon length after 24 and 48 h. **d.** Fecal morphology and volume after 24 and 48 h. **e.** Lm burden in the intestinal and extra-intestinal tissues.

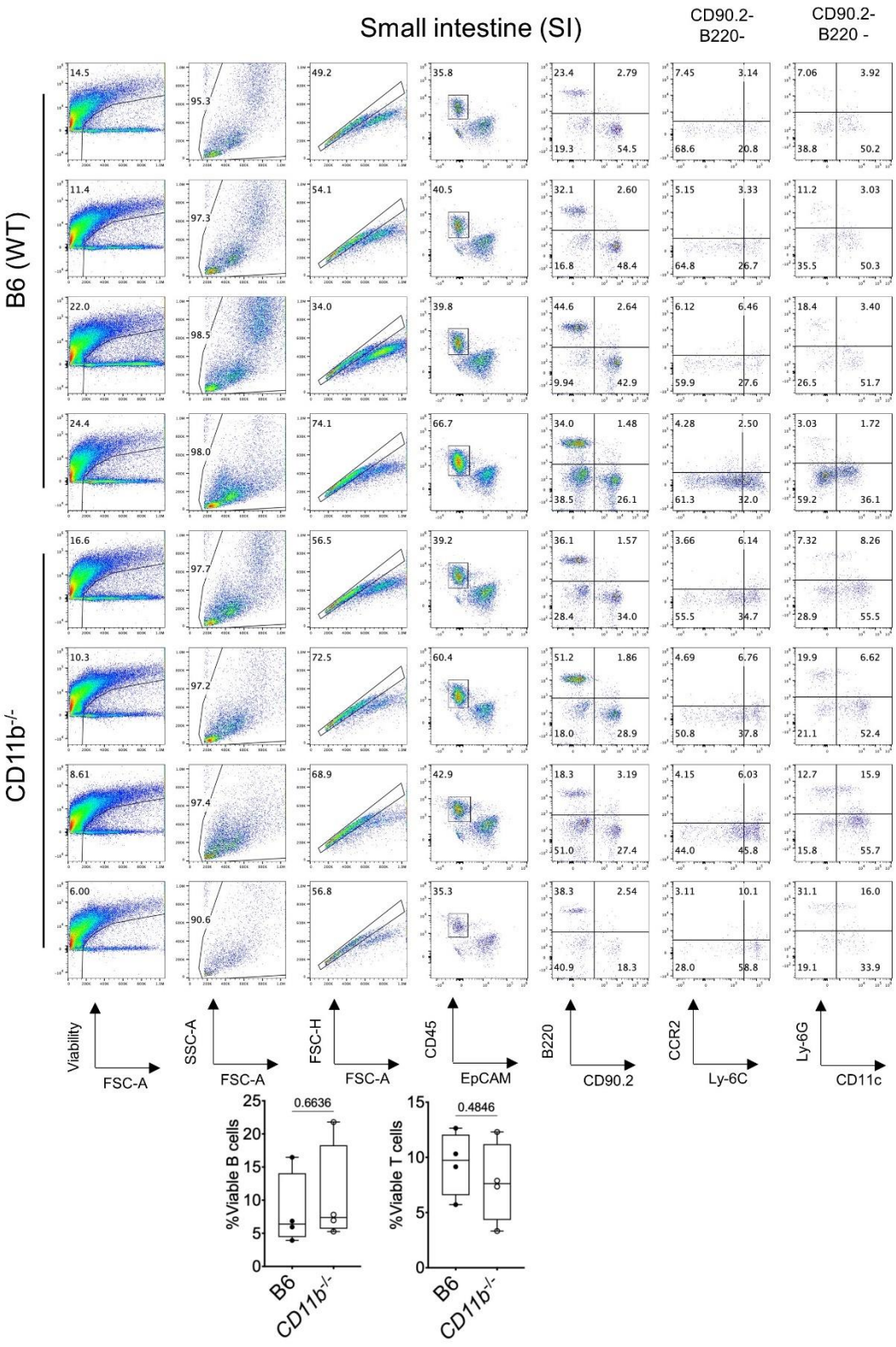

Supplementary Fig 8. Flow cytometry gating strategy and immune cell subset frequencies in the small intestine of *CD11b*$^{-/-}$ mice. Animals were infected with Lm F4244 WT at 1-2 x10^{10} CFU/mouse.

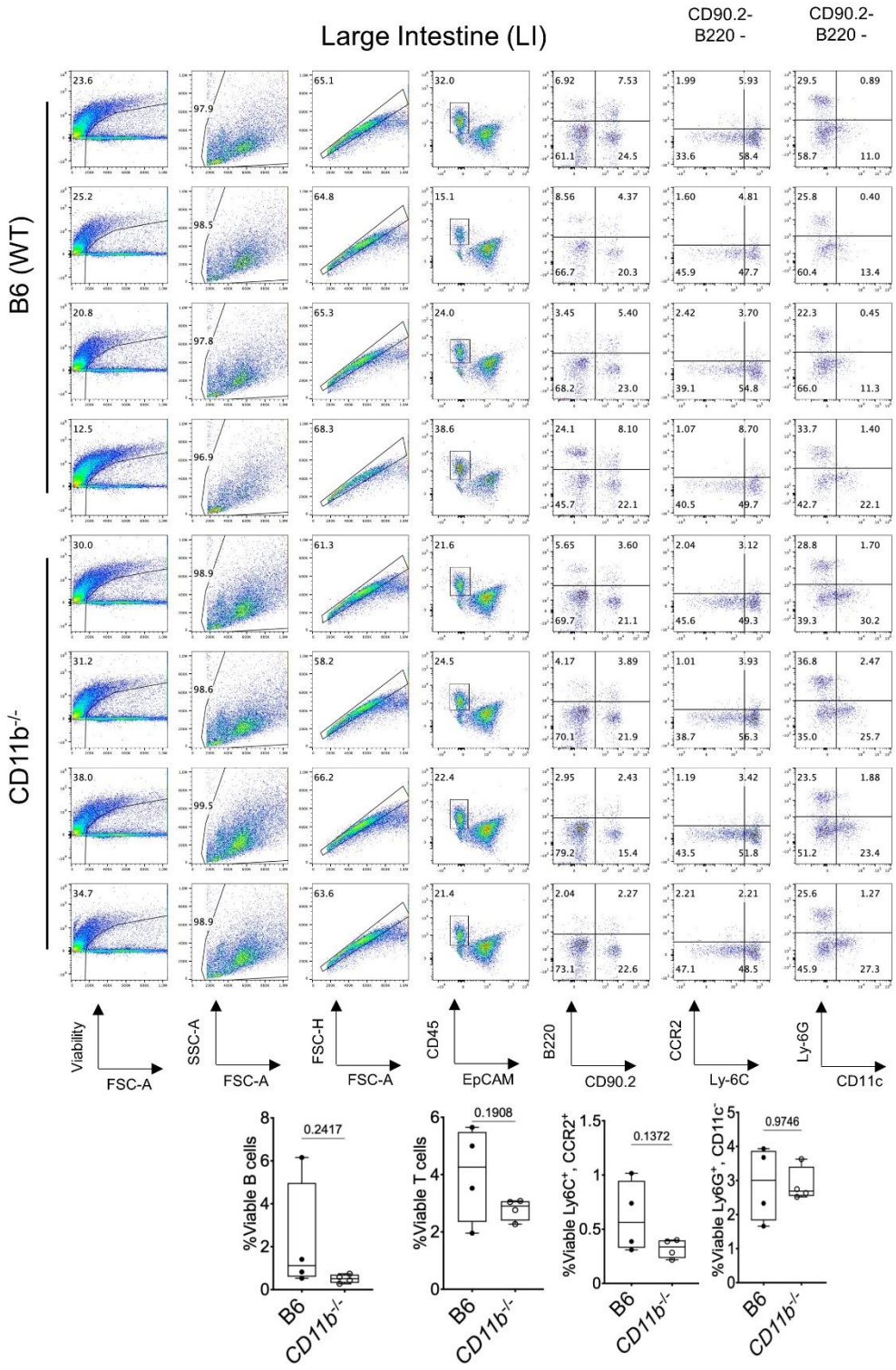

Supplementary Fig 9. Flow cytometry gating strategy and immune cell subset frequencies in the large intestine of *CD11b*$^{-/-}$ mice. Animals were infected with Lm F4244 WT at 1-2 x10^{10} CFU/mouse.

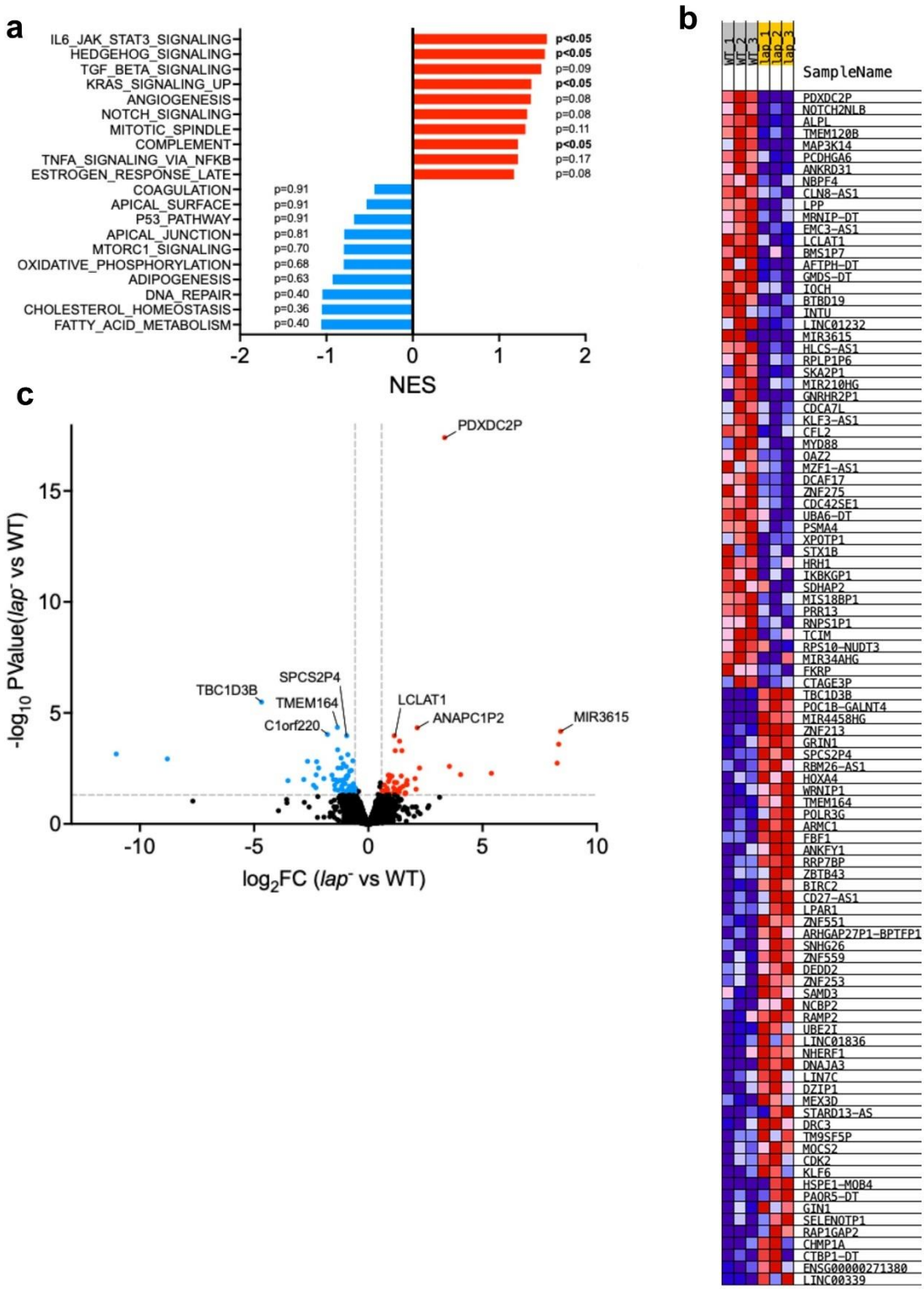

Supplementary Fig. 10. LAP-Induced Gastroenteritis is Mediated by TLR2 Signaling.
a. GESA analysis of top 10 upregulated and downregulated pathways. Significantly different pathways were bolded. **b.** RNAseq heatmap illustrating the complete list of differentially expressed genes (DEGs) in Caco-2 cells infected with Lm WT compared to the *lap*⁻ strain. **c.** Volcano plot of DEGs.

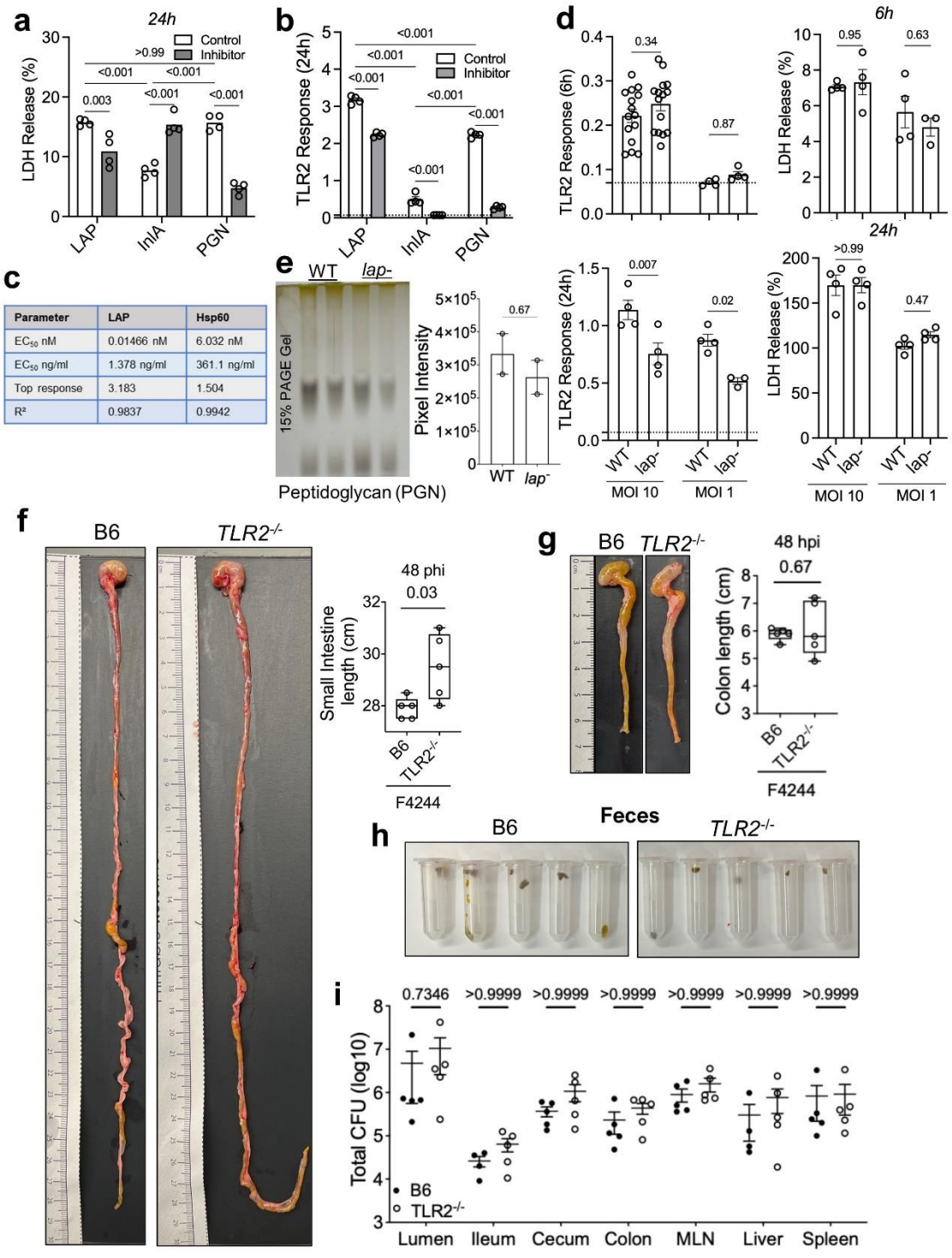

Supplementary Figure 11. LAP-Induced Gastroenteritis is Mediated by TLR2 Signaling.
a. LDH cell toxicity assay for hHEK-TLR2 reporter cell line treated with purified proteins.
b. TLR2 signal responses in hHEK-TLR2 reporter cell line with LAP, InlA and PGN and TLR2 inhibitor (TL2-C29) after 24 h.

c. TLR2 signal response (EC_{50} estimation) to variable doses of LAP and Hsp60.
d. TLR2 signal responses in hHEK-TLR2 reporter cell line treated with live Lm WT or *lap*$^{-}$ at 6 h and 24 h post-exposure and corresponding LDH release assay.
e. Wall teichoic acid (WTA) profiles of Lm WT and *lap*$^{-}$ analyzed by non-denaturing PAGE with Alcian blue staining (top) and corresponding densitometric pixel intensity analysis (bottom).
f,g. Representative images and corresponding bar plots quantifying the length of the small (stomach-ileum) (e) and large intestine (cecum-colon) (f).
h. Representative images of fecal pellets of mice infected with Lm collected at 48 hpi.
i. Lm burden in intestinal and extra-intestinal tissues at 48 hpi.

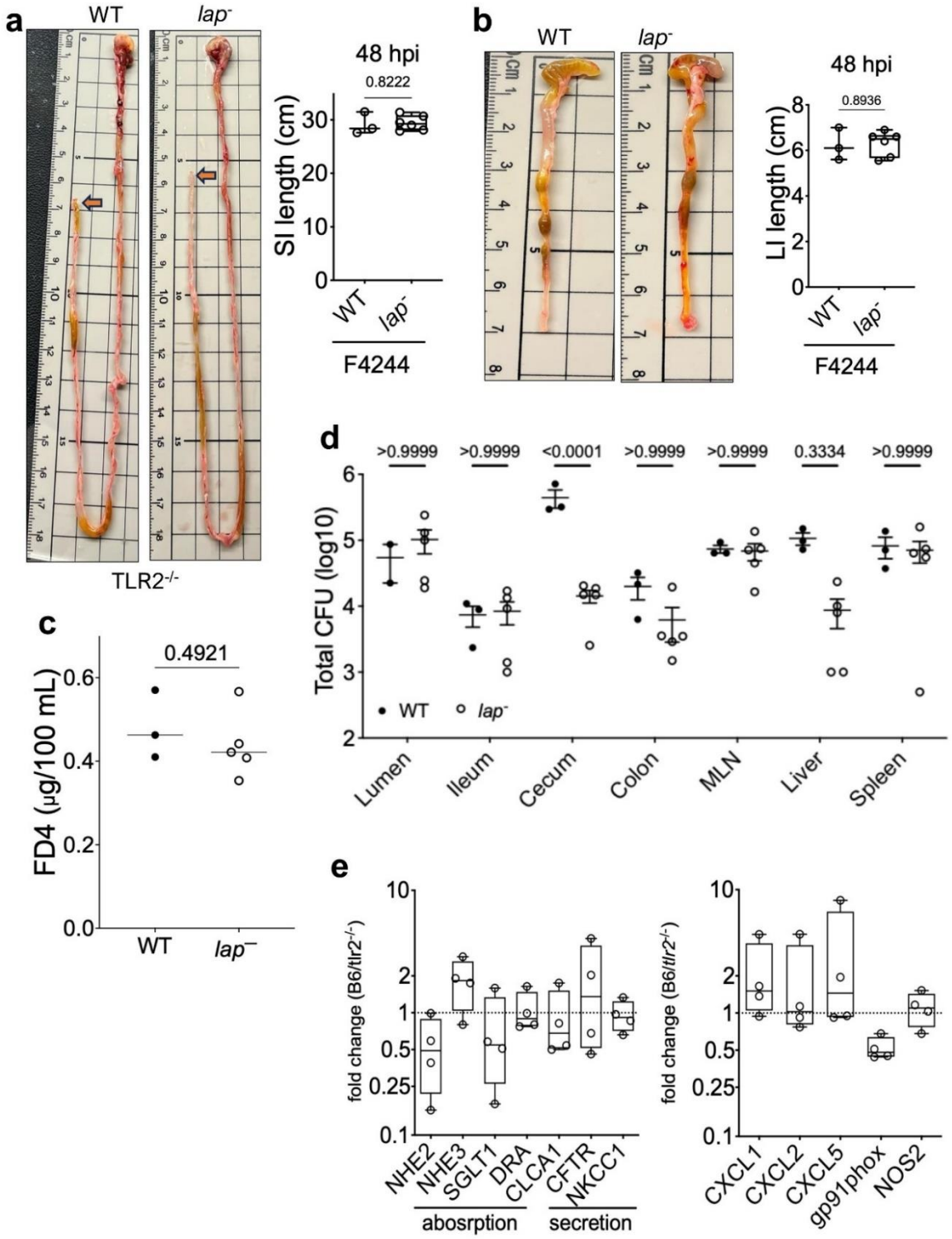

Supplementary Figure 12. LAP-Induced Gastroenteritis is Mediated by TLR2 Signaling.
a,b. Representative images and corresponding bar plots quantifying the length of the small (stomach-ileum) intestine (a) and large intestine (cecum-colon) (b) from *TLR2*$^{-/-}$ mice infected with Lm WT and the *lap*$^{-}$ strain. **c.** FD4 permeability in *TLR2*$^{-/-}$ mice infected with Lm WT and the *lap*$^{-}$ strain. **d.** Lm burden in intestinal and extra-intestinal tissue of *TLR2*$^{-/-}$ mice at 48 phi. **e.** Relative mRNA expression levels of ion channels and inflammatory markers from the ileum.

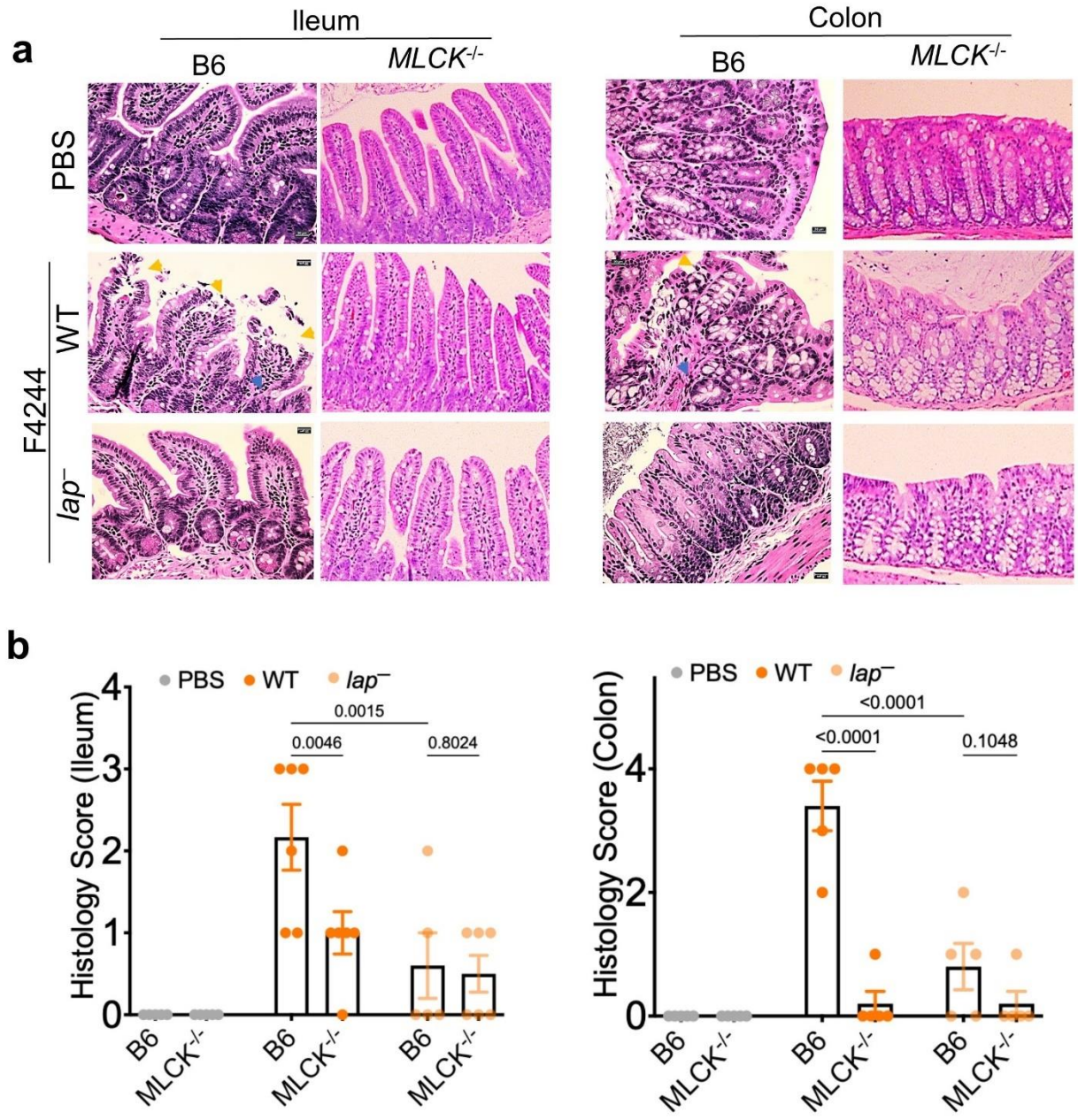

Supplementary Figure 13. MLCK deficiency preserves the paracellular gap and attenuates LAP-induced gastroenteritis.

a.b. Representative histopathology images (a) and blinded scoring data (b) from ileal and colonic tissues from Lm WT and *lap*$^{-}$ infected B6 and MLCK$^{-/-}$ mice at 48 hpi. All error bars represent SEM and are marked with p-values. All experiments were repeated at least three times unless otherwise noted.

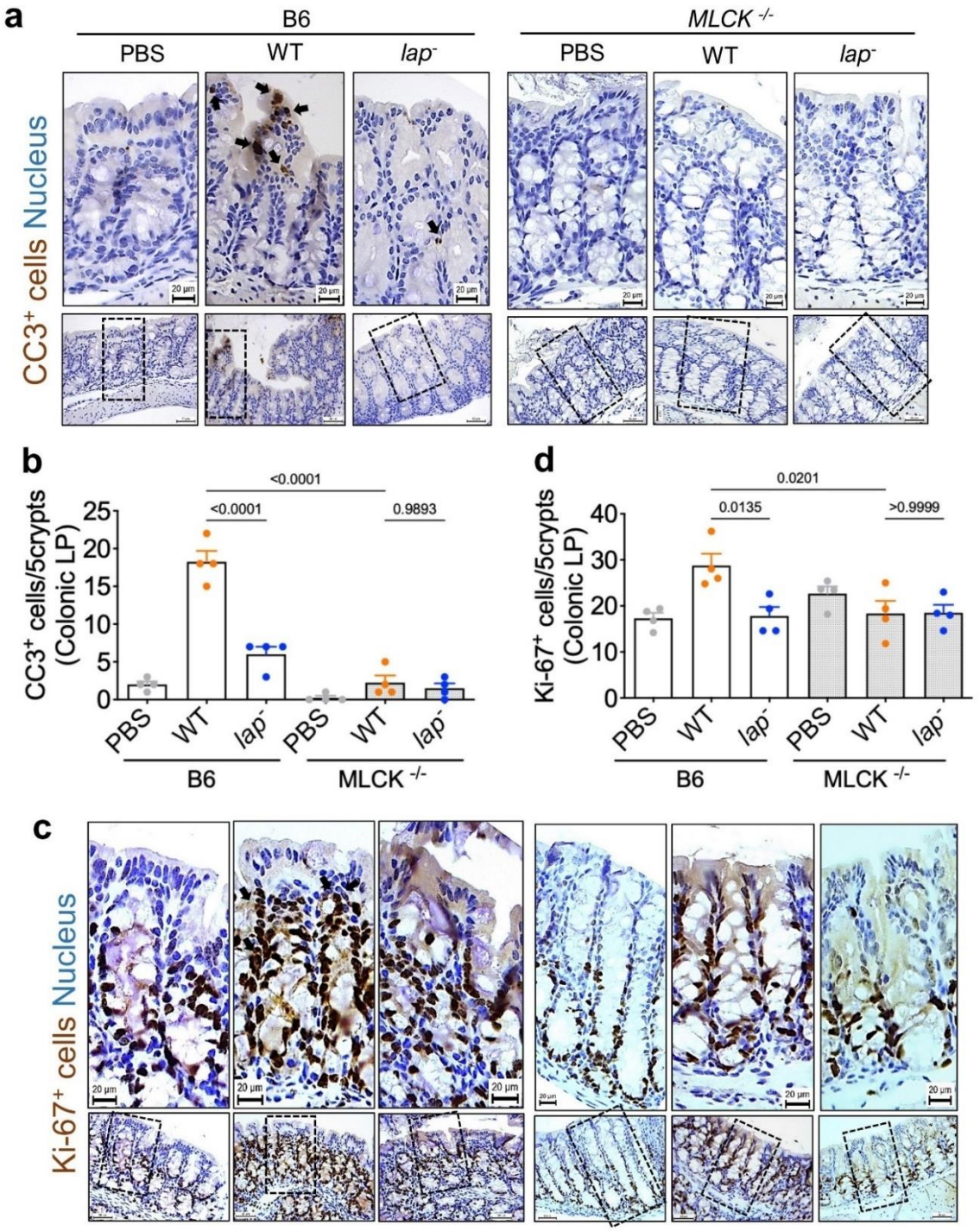

Supplementary Fig. 14. MLCK deficiency reduces Lm-induced cell death and cell proliferation at the lamina propria.

a.b. Representative colonic IHC staining of $CC3^+$ (Cleaved caspase 3) at the lamina propria and quantitative analysis showing the mean counts of $CC3^+$ (b). The nucleus was counterstained with hematoxylin. **c.d.** Representative colonic IHC staining of $Ki67^+$ at the lamina propria and quantitative analysis showing the mean counts of $Ki67^+$ (d) cells within the lamina propria. The nucleus was counterstained with hematoxylin. All error bars represent SEM and are marked with p values. All experiments were repeated at least three times unless otherwise noted.

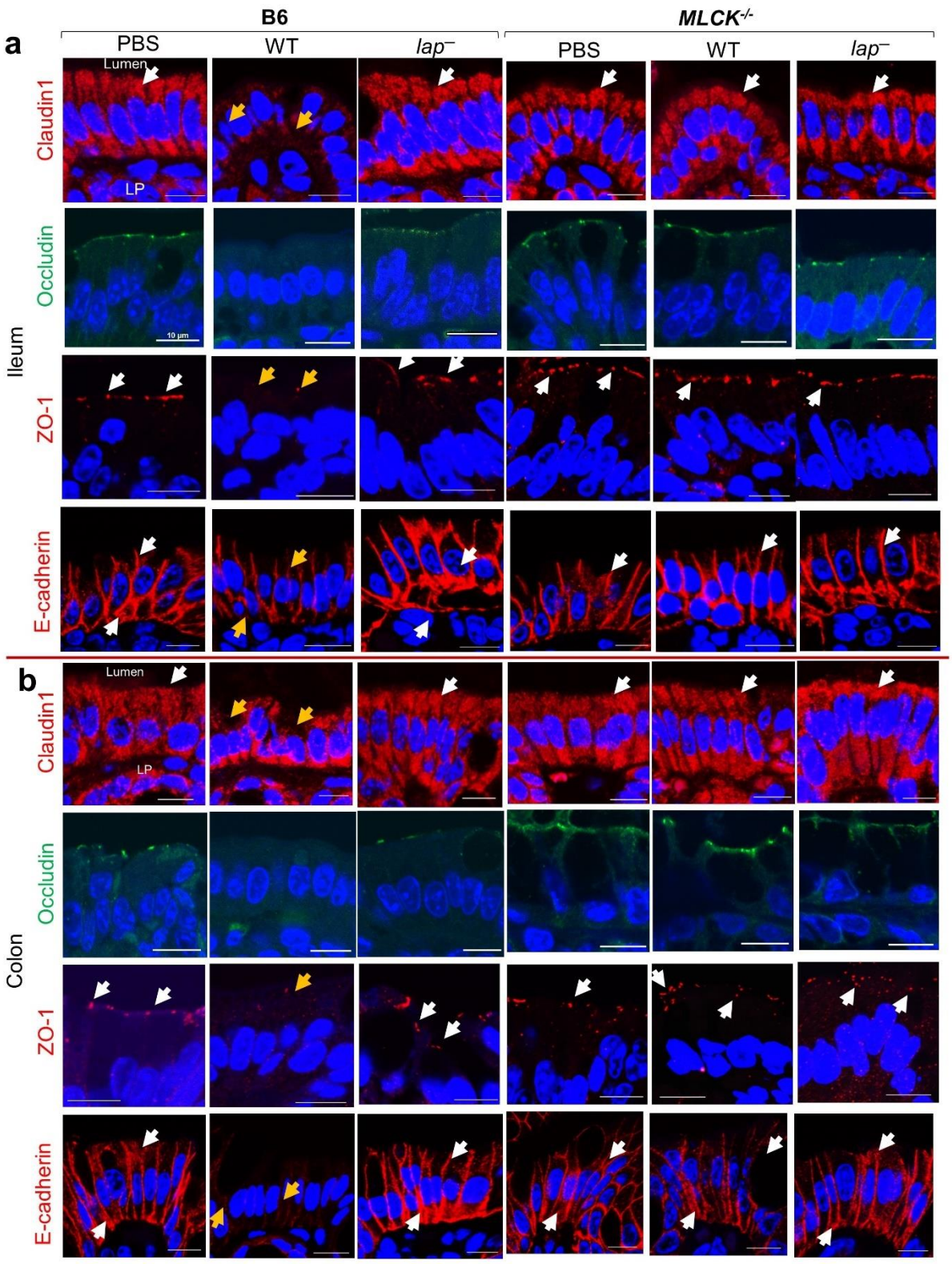

Supplementary Fig. 15. Tight junction protein profiling. Representative immunofluorescent images showing the expression and localization of the tight junction proteins Claudin-1(Red), Occludin (Green), ZO-1 (Red), and E-cadherin (Red) in the ileum (a) and colon (b). Nuclei are counterstained with DAPI (blue).

Supplementary Spreadsheet 1. Whole genome sequencing comparison of serovar 4b *Listeria monocytogenes* gastroenteritis outbreak strains (H7014 and F4244)

References

1. Bailey, T.W., do Nascimento, N.C. & Bhunia, A.K. Genome sequence of *Listeria monocytogenes* strain F4244, a 4b serotype. *Genome Announcements* **5**, e01324-01317 (2017).
2. Kim, K.-P*., et al.* Adhesion characteristics of *Listeria* adhesion protein (LAP)-expressing *Escherichia coli* to Caco-2 cells and of recombinant LAP to eukaryotic receptor Hsp60 as examined in a surface plasmon resonance sensor. *FEMS Microbiol. Lett.* **256**, 324-332 (2006).
3. Burkholder, K.M. & Bhunia, A.K. *Listeria monocytogenes* uses *Listeria* adhesion protein (LAP) to promote bacterial transepithelial translocation, and induces expression of LAP receptor Hsp60. *Infect. Immun.* **78**, 5062-5073 (2010).
4. Bai, X*., et al.* Biofilm-isolated *Listeria monocytogenes* exhibits reduced systemic dissemination at the early (12–24 h) stage of infection in a mouse model. *npj Biofilms and Microbiomes* **7**, 1-16 (2021).
5. Drolia, R*., et al. Listeria* adhesion protein orchestrates caveolae-mediated apical junctional remodeling of epithelial barrier for *Listeria monocytogenes* translocation. *mBio* **15**, e02821-02823. (2024).
6. Glomski, I.J., Decatur, A.L. & Portnoy, D.A. *Listeria monocytogenes* mutants that fail to compartmentalize listerolysin O activity are cytotoxic, avirulent, and unable to evade host extracellular defenses. *Infect. Immun.* **71**, 6754-6765 (2003).
7. Jagadeesan, B*., et al.* LAP, an alcohol acetaldehyde dehydrogenase enzyme in *Listeria* promotes bacterial adhesion to enterocyte-like Caco-2 cells only in pathogenic species. *Microbiology* **156**, 2782-2795 (2010).
8. Pandiripally, V.K., Westbrook, D.G., Sunki, G.R. & Bhunia, A.K. Surface protein p104 is involved in adhesion of *Listeria monocytogenes* to human intestinal cell line, Caco-2. *J. Med. Microbiol.* **48**, 117-124 (1999).
9. Lathrop, A.A., Banada, P.P. & Bhunia, A.K. Differential expression of InlB and ActA in *Listeria monocytogenes* in selective and nonselective enrichment broths. *J. Appl. Microbiol.* **104**, 627-639 (2008).
10. Lathrop, A.A., Bailey, T.W., Kwang-Pyo, K. & Bhunia, A.K. Pathogen-specific antigen target for production of antibodies produced by comparative genomics. *Antibody Technol. J.* **4**, 13 (2014).